

Three-dimensional dynamic Monte Carlo simulations of driven polymer transport through a hole in a wall

Shyh-Shi Chern

Department of Physics, University of Pittsburgh, Pittsburgh, Pennsylvania 15260

Alfredo E. Cárdenas

Department of Computer Science, Cornell University, Ithaca, New York 14853

Rob D. Coalson^{a)}

Department of Chemistry, University of Pittsburgh, Pittsburgh, Pennsylvania 15260

(Received 17 April 2001; accepted 21 June 2001)

Three-dimensional dynamic Monte Carlo simulations of polymer translocation through a cylindrical hole in a planar slab under the influence of an external driving force are performed. The driving force is intended to emulate the effect of a static electric field applied in an electrolytic solution containing charged monomer particles, as is relevant to the translocation of certain biopolymers through protein channel pores embedded in cell membranes. The time evolution of the probability distribution of the translocation coordinate (the number of monomers that have passed through the pore) is extracted from three-dimensional (3-D) simulations over a range of polymer chain lengths. These distributions are compared to the predictions of a 1-D Smoluchowski equation model of the translocation coordinate dynamics. Good agreement is found, with the effective diffusion constant for the 1-D Smoluchowski model being nearly independent of chain length. © 2001 American Institute of Physics. [DOI: 10.1063/1.1392367]

I. INTRODUCTION

The dynamics of single polymer translocation through a pore in a biological membrane under the influence of an external field has recently received considerable attention from both theoretical and experimental perspectives.^{1–12} Understanding this process will enable us to deepen our comprehension of many fundamental problems in cell biology, and may also contribute to the development of promising biotechnologies. For example, the process wherein a bacteriophage virus infects a bacterium by inserting its DNA into the bacterium has been studied for some time.^{13–18} Although the actual infection process is complicated by many biological factors, a simple model in which a linear polymer chain translocates through a pore embedded in a rigid and impenetrable wall provides a useful framework for understanding basic features of the threading process.¹⁰ Gene therapy^{2,3} and DNA sequencing^{4,5} are among the other potential practical ramifications associated with the problem of biopolymer translocation through protein pores. In particular, Kasianowicz *et al.*⁵ have shown that by applying an electric field across a bilayer membrane, it is possible to drive single-stranded RNA and DNA molecules through a narrow membrane-spanning channel protein. In their experiment, ion currents decreased whenever single-stranded RNA or DNA molecules entered the channel and thereby partially blocked the flow of simple ions through it. By relating the duration of the current drop to the polymer length and analyzing the

current fluctuations, they demonstrated that their technique may provide a foundation for future ultrarapid DNA sequencing.

All theoretical investigations on electric-field-driven polymer translocation through a pore in a membrane that have been carried out to date^{6–8} have been based on a 1-D drift-diffusion model. Sung and Park⁶ utilized a Fokker-Planck equation to study polymer translocation dynamics through a pore in a membrane. Muthukumar⁷ adopted a master equation approach to investigate the same problem. Lubensky and Nelson⁸ also studied 1-D drift-diffusion equations, incorporating a simple model of monomer-pore interactions, in an attempt to address the experiments done by Kasianowicz *et al.*⁵ Peskin, Oster, and co-workers¹⁹ developed a Brownian ratchet mechanism for protein translocation through biological pores using modified 1-D diffusion equations. However, none of these works address the polymer translocation in three dimensions, i.e., as the 3N-dimensional dynamics of a linear polymer chain consisting of N linked monomers. Does the motion of the 3-D polymer through the pore generate time evolution of the translocation coordinate (the number of monomers that have passed through the pore), which can be described by a simple 1-D drift-diffusion equation, as assumed in prior analyses?^{6–8} To address this question, we have carried out 3-D dynamic Monte Carlo (DMC) simulations to investigate how a polymer threads through a pore in a rigid wall.⁹ We find that it is indeed possible to capture many essential features of the translocation process using an appropriate 1-D model. Given the sensible agreement between our 3-D DMC simulations and simple theoretical expectations, we expect that we can extend these simulations to study biopolymer translocation in

^{a)}Electronic mail: coalson@pitt.edu

more realistic models of biological ion channels.

The outline of this paper is as follows. In Sec. II we present the 3-D model, our simulation technique, and 3-D simulation results for the time evolution of the distribution of the translocation coordinate and related quantities. In Sec. III we summarize salient features of a 1-D Smoluchowski equation model, originally proposed by Sung and Park,⁶ for the translocation coordinate dynamics. In Sec. IV we present the dependence of translocation time on polymer length obtained from both 3-D simulations and the 1-D Smoluchowski equation model. Section V contains discussion and conclusions.

II. MODEL, 3-D DYNAMIC MONTE CARLO SIMULATION METHODOLOGY, AND SIMULATION RESULTS

We model the dynamics of a polymer threading through a hole in a wall via 3-D dynamic Monte Carlo (DMC) simulations. By averaging over many stochastic realizations of the translocation process, we can construct spatiotemporal probability distributions of the 1-D translocation coordinate. We can then compare these distributions (and the average translocation times associated with them) to the results of 1-D drift-diffusion models, which are described in detail in Sec. III below.

A. Dynamic Monte Carlo simulations

We employ the dynamic Monte Carlo method developed by Baumgärtner and Binder^{20,21} to study our translocation problem. This methodology consists of local kink-jump moves to simulate diffusion, supplemented by a Metropolis acceptance/rejection criterion, which takes into account the effect of systematic forces acting on each particle, including both interparticle interactions and externally imposed force fields. The polymer is treated as a pearl necklace consisting of N monomeric beads, with adjacent monomers connected by a rigid rod of length l . The radius of the monomer r can be adjusted to describe the strength of the excluded volume effect. In the present study, however, we set $r=0$ for simplicity. In other words, we study (in the long chain limit) a Gaussian chain without excluded volume. Our system consists of an impenetrable wall with a small cylindrical pore in it. A potential difference is applied linearly across the wall (including the embedded pore). As shown in Fig. 1, the potential profile is given as

$$U(x,y,z) = \begin{cases} -kx, & \text{if } x \geq -L/2 \text{ and } x \leq L/2 \\ & \text{and } y^2 + z^2 \leq R_p^2, \\ -kL/2, & \text{if } x > L/2, \\ kL/2, & \text{if } x < -L/2, \\ \infty, & \text{otherwise,} \end{cases} \quad (1)$$

where we denote the thickness of the wall as L , and the radius of the pore as R_p . We adopt the values $L=l=0.2a$ and $R_p=0.1a$ for our simulations; a is our unit length and k is the strength of the applied force, which determines the tendency of the monomer to move from one side to the other. The unit of k is $k_B T/a$. For all results presented in this paper, we employ the value $k=10$. Initially, an end monomer is

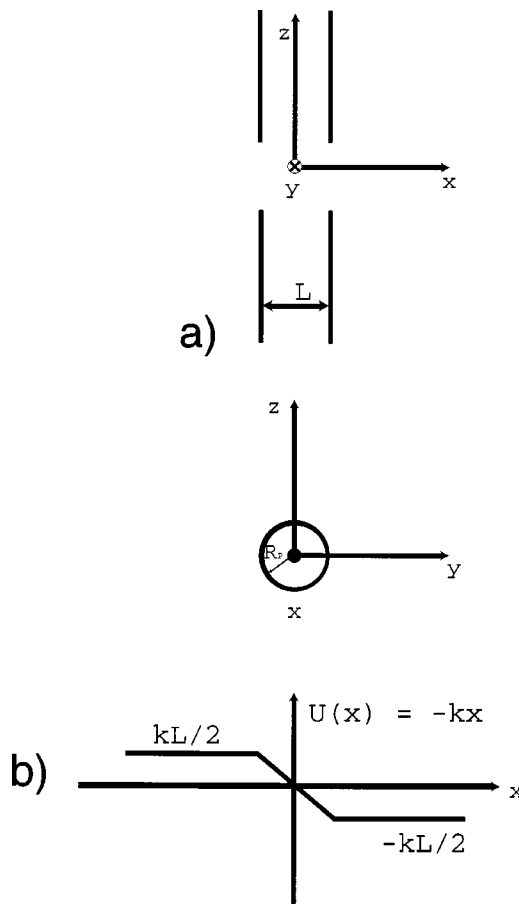


FIG. 1. An illustration of (a) the geometry of the simulation system and (b) the applied external potential profile (a linear potential ramp inside the cylindrical pore).

placed on the *trans* side and the rest of the polymer on the *cis* side²² or in the channel itself; cf. Fig. 2. The initial positions of the monomers are chosen randomly except for the constraint indicated above. We then move the polymer using the kink-jump technique: for each time step, we randomly pick the m th monomer and rotate it around the axis connecting the $(m-1)$ th and $(m+1)$ th monomers by a random angle. If an end monomer is chosen, it moves at random to a new

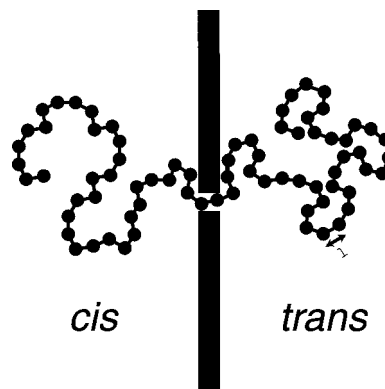


FIG. 2. An illustrative configuration of a polymer chain undergoing translocation. The polymer is initially almost entirely in the *cis* reservoir, with one monomer threaded into the *trans* reservoir. An applied external force then pushes the polymer from *cis* to *trans* sides.

position keeping the rod length fixed. The move is accepted according to the Metropolis criterion. In other words,

$$W(\alpha \rightarrow \alpha') = \begin{cases} 1, & \text{if } U_\alpha \geq U_{\alpha'}, \\ e^{-\beta(U_{\alpha'} - U_\alpha)}, & \text{otherwise,} \end{cases} \quad (2)$$

$W(\alpha \rightarrow \alpha')$ being the transition probability that a polymer in state α will be in state α' at the next step. As usual, $\beta = 1/k_B T$, while U_α and $U_{\alpha'}$ are the potential energies of states α and α' , respectively.

In recent work we have used the kink-jump Monte Carlo technique to investigate the equilibrium configurations sampled by a polymer translocating through a narrow pore between two confining (spherical) cavities.²³ Here we wish to study kinetics of transport through such a pore, in the biologically relevant case where there is no confinement on either side of the dividing wall. Following standard polymer simulation methodology,^{20,21,24} we define a Monte Carlo microstep t_{MC} as the time required to move one monomer from the state α to the state α' . Then the ‘‘sweep time’’ (or Monte Carlo step) $t_{sweep} = t_{MC}/N$ becomes our time unit for the underlying physical system.^{21,25}

Baumgärtner has shown²¹ that the kink-jump Monte Carlo algorithm, when used to simulate the dynamics of a single linear polymer chain in an isotropic medium (with no external forces), reproduces many signatures of the Rouse model,²⁶ i.e., a Gaussian chain model of the polymer that excludes complications such as hydrodynamic coupling. To test the kink-jump Monte Carlo algorithm code used in the present work, we performed test simulations for the same problem. We found that predictions of the Rouse model were indeed recovered from our simulation data. For example, we examined the end-to-end distance d_e and found that it obeyed the expected relation $d_e^2 = Ml^2$, with M being the number of links, i.e., $M = N - 1$. Also, the displacement of the position of the center of mass was found to be diffusive, i.e., the mean-square displacement grew linearly with time for sufficiently long times, as predicted by the Rouse model. The dependence of the center of mass diffusion constant on polymer chain length was computed. According to the Rouse model, this diffusion constant should decrease as M^{-1} , and indeed this behavior was observed in our test simulations.

The model adopted in this work is directly inspired by the experiments of Kasianowicz *et al.*,⁵ who applied an electric field across a lipid bilayer membrane in order to drive single-stranded DNA and RNA through an aqueous pore in the membrane. The pore is generated by a protein channel (specifically, α -hemolysin), which inserts into the membrane in a perpendicular, membrane-spanning orientation. The DNA is negatively charged due to phosphate groups from which the counterions have dissociated. The water solvent contains dissolved salts (electrolytes). The electric field was applied using microelectrodes positioned far from the channel (pore) entrance.

We connect the biological system just outlined to the simulation system described above by the following arguments. The electrolyte ions are expected to screen the charges on the DNA nucleotides (monomers), so that the interactions between nonbonded monomers become short range in character. Specifically, they are reasonably well de-

scribed by exponentially screened Coulomb potentials,²⁷ although the details of this short range potential are not critical. It could be modeled qualitatively as an excluded volume potential that prevents the overlap of finite-radius monomers. As noted above, we have, for simplicity, suppressed this effect in the numerical simulations to be presented here by setting the effective monomer radius to zero.

The electrolyte ions also screen the electric field generated by the electrodes. Essentially this field is zero inside the electrolyte solution (i.e., the electrolyte region on either side of the membrane is an equipotential region). If there were no pore and no monomer, a constant electric field would exist in the membrane region. The presence of a small pore with or without a polymer chain threaded through it is assumed to modify this situation only slightly, and hence negligibly. Thus, we assume the electric potential felt by each monomer is constant in each reservoir and drops linearly across the pore. The overall model system then corresponds to non-charged monomers moving in an external potential field given by Eq. (1).

Muthukumar has recently studied a related problem using a similar model and simulation methodology.¹⁰ He has calculated the escape kinetics of a linear polymer chain from a hole in a spherical cavity. In the present work we focus on the translocation of a polymer chain through a hole in a flat wall, when driven by an electric field that is applied across the thickness of the wall. We seek primarily to investigate the level of validity of 1-D drift-diffusion or Smoluchowski equation models of the translocation dynamics by a comparison to full 3-D polymer dynamics, as is discussed in detail below.

B. DMC simulation results: Translocation probability distributions

The initial condition for the simulation consists of a barely threading polymer such that one monomer is on the *trans* side, while all the other monomers are either in the channel or on the *cis* side. Stochastic DMC dynamics is then carried out using the external driving force described above until the polymer either retracts to the *cis* side or translocates completely to the *trans* side. Either event signals the end of the simulation. This calculation is repeated many times and statistics concerning the number of monomers n on the *trans* side (i.e., the translocation coordinate) as a function of elapsed time are collected, resulting in a synthesis of the translocation probability distribution $P(n, t)$, normalized (for convenience) to unit integrated strength at $t=0$ [essentially, $P(n, 0) = \delta(n - n_0)$, with $n_0 = 1$].

Plots of $P(n, t)$ for polymer chains of length $N = 50, 100, 150, 200$ are shown in Figs. 3 and 4. Since both the $n=0$ and $n=N$ configurations are ‘‘lost’’ from the pore, the distribution $P(n, t)$ is characterized by absorbing boundary conditions at both end points. Thus, the ensemble loses members at both $n=0$ and $n=N$ ends, and $P(n, t) \rightarrow 0$ at large t . This behavior is illustrated by computing the survival probability:

$$p_{\text{surv}}(t) \equiv \int_0^N P(n, t) dn, \quad (3)$$

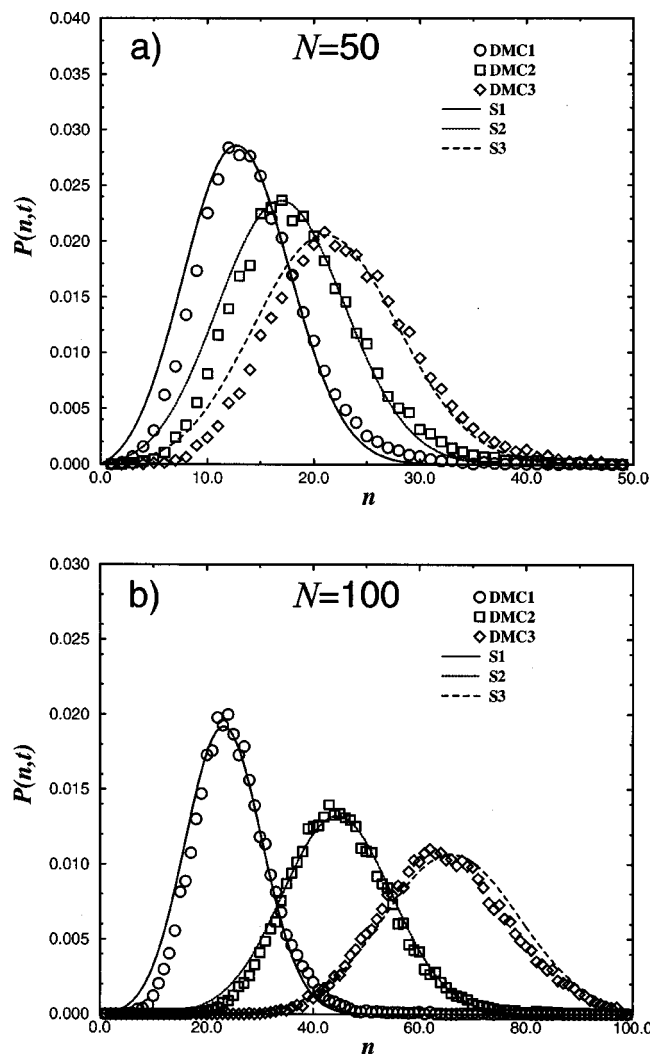


FIG. 3. (a) The probability distribution of the translocation coordinate n at different times for a chain with $N=50$. S denotes a 1-D Smoluchowski equation solution (cf. Sec. III), and DMC denotes data from our 3-D dynamic Monte Carlo simulations. $S1$, depicted by a straight line, represents probability distribution $P(n,t)$ at $Dt=13.5$, with $D=0.0135$ here and in all subsequent figures. $S2$, depicted by a dotted line, represents $P(n,t)$ at $Dt=18.9$. $S3$, depicted by a dashed line, represents $P(n,t)$ at $Dt=24.3$. DMC1, depicted by circles, represents $P(n,t)$ at $Dt=13.5$. DMC2, depicted by squares, represents $P(n,t)$ at $Dt=18.9$. DMC3, depicted by diamonds, represents $P(n,t)$ at $Dt=24.3$. (b) The same as in (a), except here $N=100$. The three relevant times, coinciding with the leftmost (earliest time) to rightmost (latest time) probability distributions, are $Dt=27.0, 54.0, 81.0$. Note that the error bars are not shown in this and all subsequent figures because they are roughly the size of the symbols.

plots of which are shown in Figs. 5 and 6. The time integral of the survival probability is the mean first passage time, which provides a measure of how long the polymer dwells in the pore (see below).

The simulation data presented in this work reflects a statistical average over 50 000 repetitions of the translocation process for the $N=50$ chain and 80 000 repetitions each for the $N=100, 150, 200$ chains. For all data points presented here, the error bars are not much larger than the size of the plotting symbols, and hence are suppressed for the sake of clarity.

Note that all the 3-D simulation data sets presented in

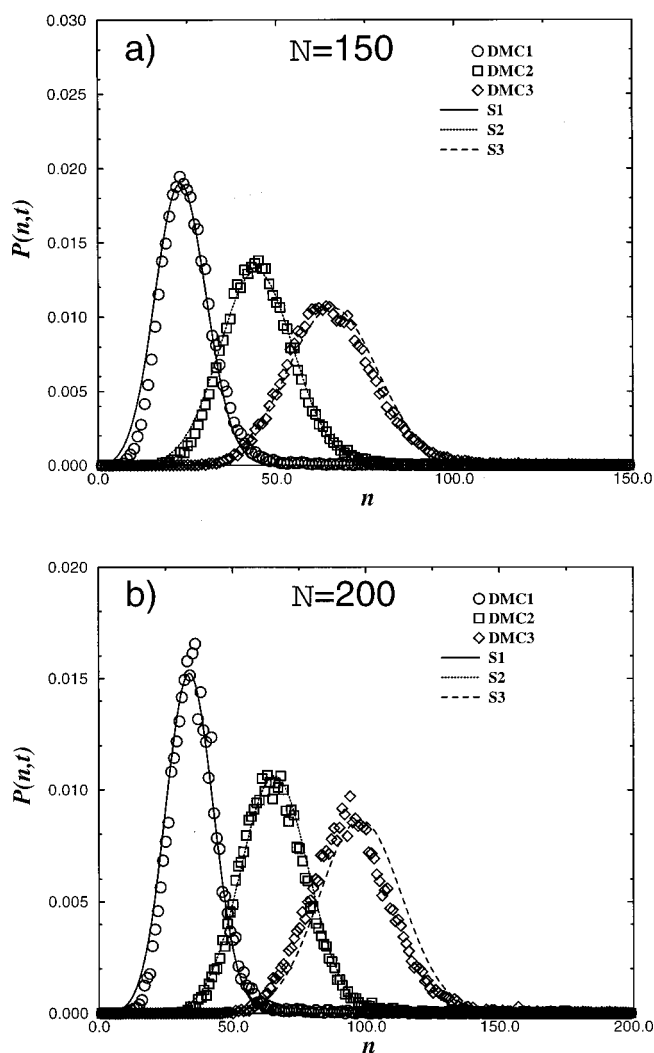


FIG. 4. (a) The same as in Fig. 3(a), except $N=150$ here. The three relevant times, coinciding with the leftmost (earliest time) to the rightmost (latest time) probability distributions, are $Dt=27.0, 54.0, 81.0$. (b) The same as in Fig. 3(a), except $N=200$ here. The three relevant times, coinciding with the leftmost (earliest time) to the rightmost (latest time) probability distributions, are $Dt=40.5, 81.0, 121.5$.

Figs. 3 and 4 are “fit” by appropriate smooth curves. These curves depict results obtained from a 1-D Smoluchowski equation model of the translocation process. Moreover, the effective 1-D potential and diffusion constant used in the 1-D Smoluchowski equation calculations are the same for all polymer lengths studied. Details of this 1-D model are provided next.

III. 1-D SMOLUCHOWSKI EQUATION MODEL OF THE TRANSLOCATION PROCESS

A. Formulation of the model

In recent work,^{6–8} the 3-D polymer translocation problem (involving $3N$ dynamical variables) has been studied by invoking a reduced 1-D model of the translocation process. In this model, the dynamical variable is the “translocation coordinate” n (*vide supra*). In the treatment given by Sung

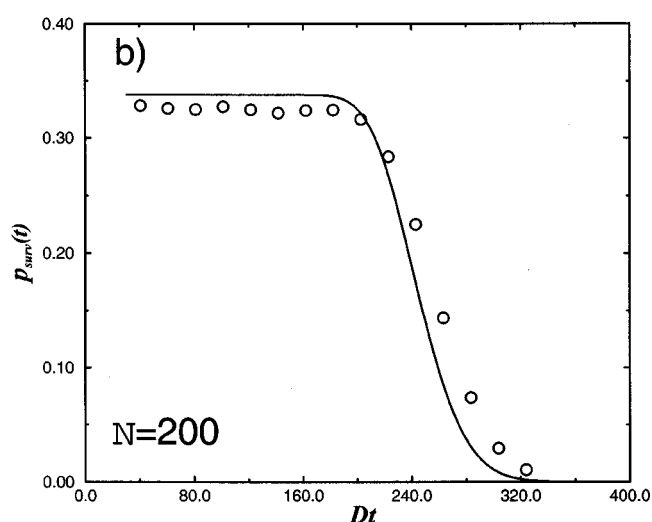
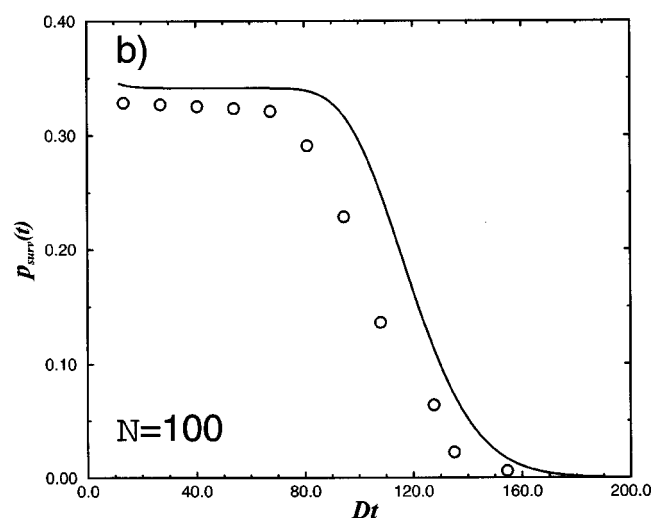
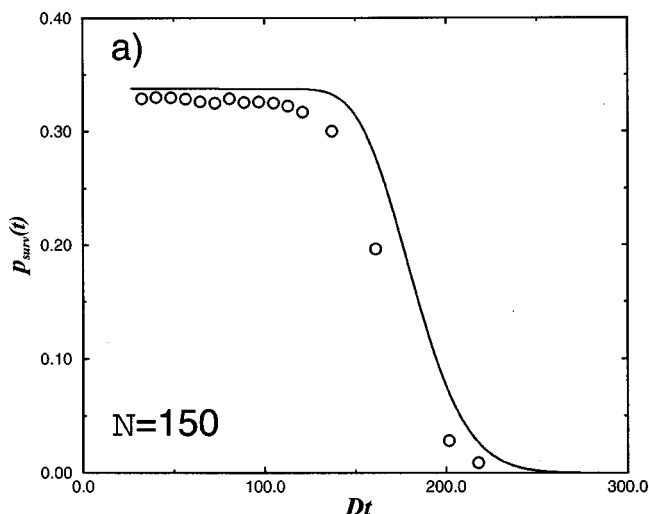
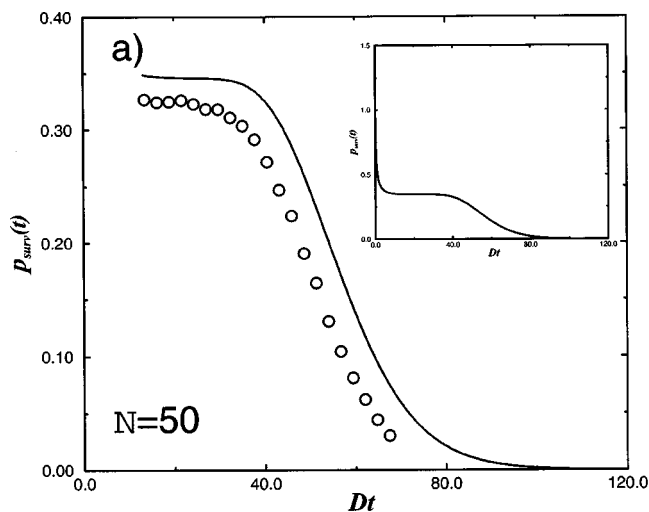


FIG. 5. (a) The survival probability $p_{\text{surv}}(t)$ vs time Dt for $N=50$. The straight line represents the results from the 1-D Smoluchowski equation solver and the circles represent those from the 3-D DMC simulations. The inset shows the early-time dynamics of $p_{\text{surv}}(t)$ calculated according to the 1-D Smoluchowski equation. (b) $p_{\text{surv}}(t)$ vs Dt for $N=100$. The straight line represents the results from the 1-D Smoluchowski equation solver and the circles represent those from the DMC simulations.

FIG. 6. (a) The same as Fig. 5(b), except $N=150$ here. (b) The same as Fig. 5(b), except $N=200$ here.

and Park,⁶ the probability distribution of the translocation coordinate $P(n,t)$ was assumed to obey the following 1-D Smoluchowski equation:

$$\frac{1}{D} \frac{\partial}{\partial t} P(n,t) = \frac{\partial}{\partial n} \left(\frac{\partial}{\partial n} + \beta \frac{\partial V(n)}{\partial n} \right) P(n,t). \quad (4)$$

In this expression, $V(n)$ is the effective potential (actually a free energy) and D a diffusion constant. Sung and Park took $V(n)$ to be the sum of two terms:

$$V(n) = \frac{1}{2} k_B T \ln[n(N-n)] - nF. \quad (5)$$

The first term on the rhs describes the contribution to the free energy due to the conformational entropy of a Gaussian chain threaded through a hole in an impenetrable wall with n monomers on the *trans* side and $N-n$ monomers on the *cis* side. The second term, which is linear in n , accounts for the intrinsic chemical potential difference between the *cis* and

trans sides of the wall. (This potential is modulo an overall shift constant that does not affect any physical properties and hence can be set to zero.) Details of how the diffusion constant D and “driving force” F are chosen to best capture the $3N$ -coordinate dynamics in terms of the 1-D Smoluchowski description just outlined are provided below.

B. Consequences of the model: A formula for the mean first passage time

A widely utilized measure^{28,29} of the translocation time (how long the polymer threads the pore before exiting completely on either the *cis* or *trans* sides) is the mean first passage time, which is defined in terms of the survival probability [Eq. (3) above] as

$$\tau \equiv \int_0^{\infty} dt p_{\text{surv}}(t). \quad (6)$$

One advantage of this definition of translocation time is that, for a distribution evolving according to a 1-D Smoluchowski equation (4), it is possible to derive a simple quadrature formula for the mean first passage time that is valid for any

potential $V(n)$. The details of this formula depend on the boundary conditions at the end points of the n -space interval.

Given dynamics according to the Smoluchowski equation (4), with initial conditions that correspond to delta function localization at $n = n_0$, i.e., $P(n, 0) = \delta(n - n_0)$, it can be shown²⁸ that the mean first passage time $\tau(n_0, N)$ defined in Eq. (6) satisfies a linear second-order differential equation with two integration constants that are determined by the relevant boundary conditions. In particular, if $P(0, t) = P(N, t) = 0$ (absorption at both ends of the active space, to be denoted as “double-absorption” boundary conditions), one finds

$$D\tau(n_0, N) = [f_1(n_0)f_2(N) - f_1(N)f_2(n_0)]/f_1(N), \quad (7)$$

where

$$f_1(n) \equiv \int_0^n dn' e^{\beta V(n')}; \quad (8)$$

$$f_2(n) \equiv \int_0^n dn' e^{\beta V(n')} \int_0^{n'} dn'' e^{-\beta V(n'')}.$$

If, on the other hand, the relevant boundary conditions are $P(N, t) = 0, dP(0, t)/dt = 0$ (absorption at one boundary, reflection at the other, or “absorption–reflection” boundary conditions), one obtains

$$D\tau(n_0, N) = f_2(N) - f_2(n_0). \quad (9)$$

While the formula corresponding to reflection at $n = 0$ has been used in most previous analyses of the polymer translocation problem (with an initial condition corresponding to the population just inside the reflecting boundary), our simulation results show that in the 3-D model adopted in the present work, double-absorption boundary conditions are appropriate. Physically, the polymer chain, which is barely threaded inside the *trans* region, can retract completely into the *cis* region. There are no forces preventing it from doing so, and once it retracts completely it is “lost.” This is precisely the statement that there is an absorbing boundary at $n = 0$.

For a general potential $V(n)$, the functions f_1 and f_2 can be evaluated by (trivial) numerical integration. For the case of a linear potential ramp [the second term on the rhs of Eq. (5)], an analytical evaluation can be obtained:

$$f_1(n) = \frac{1}{\beta F} (1 - e^{-\beta F n}); \quad (10)$$

$$f_2(n) = \frac{1}{\beta F} \left(n - \frac{1}{\beta F} (1 - e^{-\beta F n}) \right).$$

One then finds in the large N limit ($\beta F N \gg 1$) the following results. For absorption–reflection boundary conditions,

$$D\tau(n_0, N) = N/\beta F + C, \quad (11)$$

where C is a constant, dependent on n_0 but independent of N . For double-absorption boundary conditions,

$$D\tau(n_0, N) = (1 - e^{-\beta F n_0})N/\beta F + C. \quad (12)$$

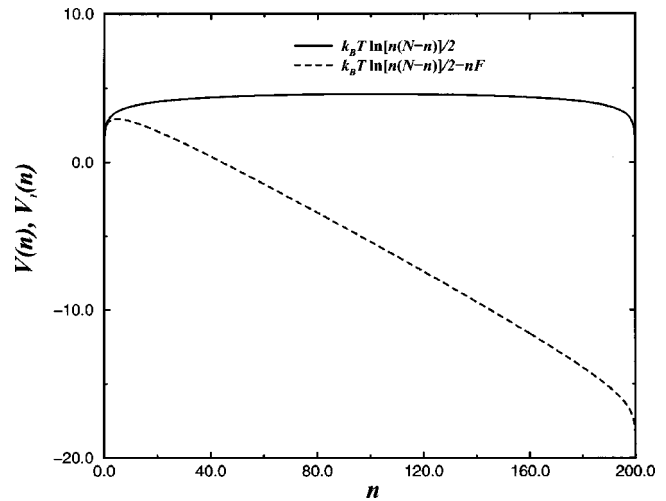


FIG. 7. Sung–Park potential $V(n) = V_1(n) - nF$, with $V_1(n) = \frac{1}{2}k_B T \ln[n(N-n)]$. Here $N = 200$ and $F = 0.1$ in units of $k_B T$.

C. Fitting D and F in the 1-D Smoluchowski model

A plot of the configurational entropy term in the Sung–Park potential and the complete Sung–Park potential (sum of configurational energy term plus linear ramp term) is shown in Fig. 7. Note that the configurational entropy contributes to the driving force only at the edges of the n -space interval (i.e., when the polymer is barely threaded through the pore or when it is almost completely through the pore). In the middle of the interval, the linear ramp term dominates.

Furthermore, we note from the 3-D translocation data (cf. Figs. 3 and 4) certain general trends in the dynamics. At short times, the polymer can fully retract to the *cis* side, at which time it is lost forever (“absorbed at $n = 0$ ”). This process does occur in our simulations, as illustrated in the inset to Fig. 5(a). For those chains out of the ensemble of runs that are performed that are pushed into the center of the interval (become significantly threaded), the linear driving force, proportional to F , drives them inexorably toward the *trans* side. Eventually they exit from this side (are “absorbed at $n = N$ ”). Thus, there is a plateau region where the time evolution of the distribution $P(n, t)$ is governed predominantly by the linear ramp term in the Sung–Park potential.

The propagation of a 1-D probability distribution according to the Smoluchowski equation is easy to determine when the driving potential is linear (constant force), particularly when the initial distribution is Gaussian. In this case the distribution remains Gaussian for all times, as described by two time-dependent parameters: the center or expectation value of the distribution, and its width. Indeed, we see from our 3-D simulations that in the plateau region this behavior is observed to a good approximation. That is, the distribution enters the region as a Gaussian. It then continues to propagate as a Gaussian, moving toward the $n = N$ end point and spreading out as it goes. When its forwardmost edge reaches $n = N$ it is influenced by the entropic (nonlinear) term in the potential, and ultimately it is absorbed at $n = N$, so the linear ramp/Gaussian distribution scenario breaks down. But in the plateau region it is rather good.

Two technical details about the time evolution of a

Gaussian distribution in a linear potential allow us to systematically extract values of D and F that can then serve as a guide for final “fine tuning” of these parameters to optimally fit the 3-D datasets. Given a particle³⁰ moving along the n coordinate in a linear potential $-Fn$ (corresponding to a constant driving force F), then a distribution that is Gaussian at t_0 remains Gaussian for all $t > t_0$, i.e.,

$$P(n,t) = \frac{1}{\sqrt{2\pi\sigma^2(t)}} e^{-(n-n_t)^2/2\sigma^2(t)}, \quad (13)$$

where

$$\sigma^2(t) = \sigma_0^2 + 2D(t-t_0); \quad n_t = n_0 + v_0(t-t_0), \quad (14)$$

and $v_0 = FD/k_B T$. Hence, a plot of $\sigma^2(t)$ increases linearly with time, as does a plot of n_t . This provides a way to extract values of D and F from the time evolution of such probability distributions.

Specifically, for a given chain length polymer, we measure the widths of the distributions obtained in the plateau regions from the 3-D simulations, and then plot $\sigma^2(t)$ vs t . Results are shown in Figs. 8 and 9. Note that these plots are, in fact, linear to a reasonable approximation. Next, we compute and plot n_t vs t for the same simulation data. These plots are also shown in Figs. 8 and 9. Again, they are approximately linear. Thus we can extract first D (from the time evolution of the distribution width) and then F (from the time evolution of the expectation value of the distribution). (Note: the units of D are $[n^2]/[t]$ and those of F are $[T]/[n]$.)

Results of least-squares fits to these curves are shown in Table I. It is clear that both D and F are essentially independent of polymer chain length, a point that is discussed at some length below.

D. Relationship of F to kL

The fact that we obtain (cf. Table I) approximately the same value of F for all polymer lengths studied is not unexpected, since F correlates with the energy change associated with the net addition of one monomer to the *trans* reservoir (and corresponding removal of one monomer from the *cis* reservoir). Further details of this correspondence are described next.

We expect the effective force F that enters into the 1-D translocation coordinate Smoluchowski equation (4) to be at least approximately proportional to the systematic force k that is applied across the pore region. To attempt a more precise identification, consider the diagram in Fig. 10. This shows a configuration with n monomers on the *trans* side, i.e., the translocation coordinate is n . As indicated there, the pore is long enough to hold several (n_p) monomers (for the parameters used in our study, $n_p \approx 2$). Due to the rigid rods connecting the monomers, configurational fluctuations inside the pore “tube” are restricted. As a crude description of the passage of monomers through the pore, we can consider an n_p -site model. That is, the n_p monomers that are in the pore are locked at positions x_1, x_2, \dots, x_{n_p} , respectively. The remaining monomers are either on the *cis* or the *trans* side of

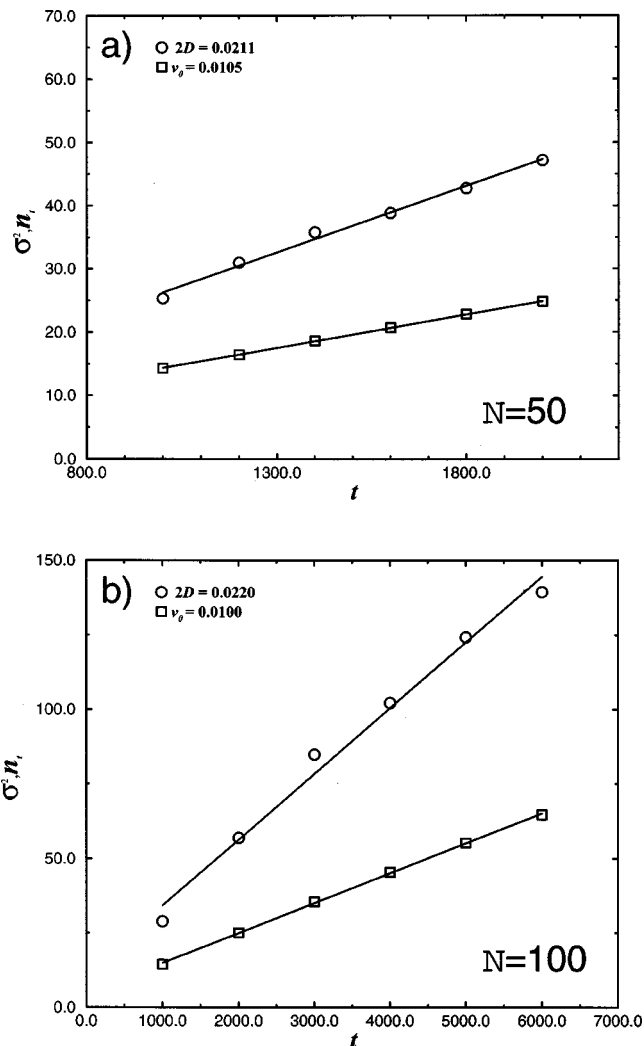


FIG. 8. (a) σ^2 and n_t vs t for $N=50$. σ^2 vs t is depicted by circles; its slope $2D$ is 0.0211. n_t vs t is depicted by squares; its slope v_0 is 0.0105. (b) σ^2 and n_t vs t for $N=100$. σ^2 vs t is depicted by circles; its slope $2D$ is 0.0220. n_t vs t is depicted by squares; its slope v_0 is 0.0100.

the wall. Given the microscopic potential in Eq. (1), the total potential energy of the configuration indicated in Fig. 10 is

$$U_{\text{tot}}(n) = (N - n - n_p)kL/2 - k \sum_{j=1}^{n_p} x_j - nkL/2. \quad (15)$$

Now, consider a shift in the chain by one monomer, so that there are $n+1$ monomers on the *trans* side. For this case,

$$U_{\text{tot}}(n+1) = (N - n - n_p - 1)kL/2 - k \sum_{j=1}^{n_p} x_j - (n+1)kL/2. \quad (16)$$

(This pattern is broken at the very beginning and end of the translocation process, when n or $N-n$ are less than about n_p . We consider chains with $N \gg n_p$, so that this edge effect can be neglected.) Thus, we obtain

$$U_{\text{tot}}(n+1) - U_{\text{tot}}(n) = -kL, \quad (17)$$

which is consistent with a translational “chemical potential” of $-kL$, i.e., $V(n) = -kLn$ (plus the entropic free en-

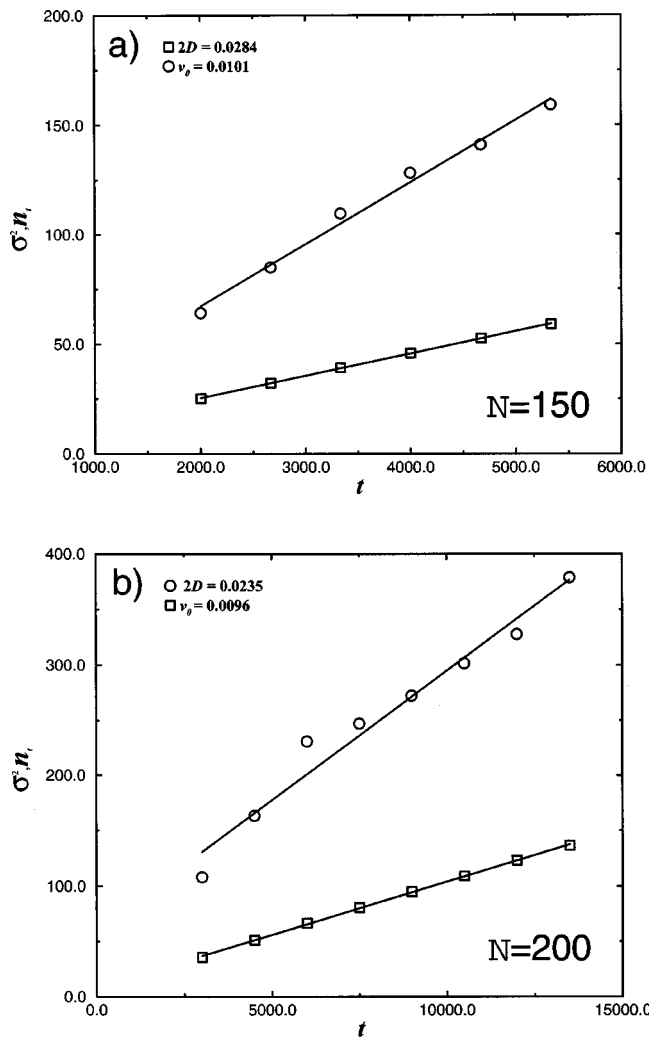


FIG. 9. (a) σ^2 and n_i vs t for $N=150$. σ^2 vs t is depicted by circles; its slope $2D$ is 0.0284. n_i vs t is depicted by squares; its slope v_0 is 0.0101. (b) σ^2 and n_i vs t for $N=200$. σ^2 vs t is depicted by circles and its slope $2D$ is 0.0235. n_i vs t is depicted by squares; its slope v_0 is 0.0096.

ergy associated with configurations accessible to the parts of the chain that are free to move in either *cis* or *trans* regions). In other words, we make the identification $F=kL$.

For the parameter values adopted in this study $kL=2.0$, whereas the best-fit value for F obtained from the 3-D translocation simulation data via the method described above is approximately 0.8 (see below). Thus, the argument just presented for connecting the microscopic potential U to the effective translocation potential V is qualitatively born out. At the same time, it is important to stress that this argument,

TABLE I. Values of D and F in Eq. (14) that best fit the plots of $\sigma^2(t)$ vs t and n_i vs t of the 3-D simulations for the different chain lengths N considered.

N	D	F
50	0.0105	0.995
100	0.0110	0.909
150	0.0142	0.711
200	0.0127	0.817
Average	0.0121	0.858

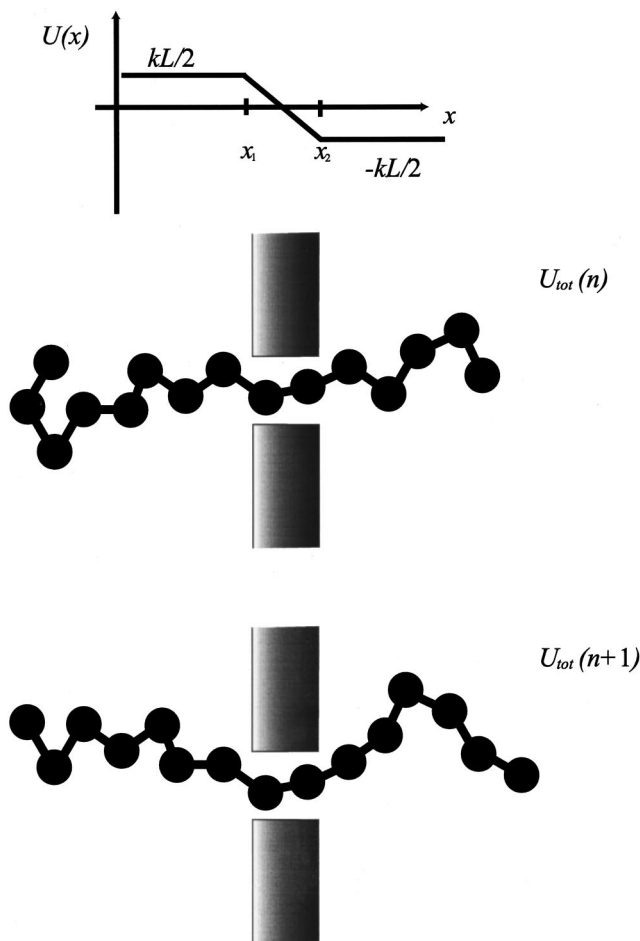


FIG. 10. An illustration of a two binding site model with $N=15$ and $n=5$.

and in particular the restriction to a single n_p -site configuration inside the channel, is crude, especially for the rather “wide channel” configuration (channel width equal polymer rod length) adopted in the present work. Hence a discrepancy at the quantitative level, as observed here, is not unexpected.

E. Numerical solution procedure for the 1-D Smoluchowski equation and results for the Sung–Park potential

To obtain numerical solutions to the 1-D Smoluchowski potential for an arbitrary system potential $V(n)$, we discretize the “spatial” derivatives (i.e., those corresponding to the translocation variable n) using the simplest possible symmetric second-order differencing scheme. We then have a set of coupled ordinary differential equations (ODEs) in the time coordinate. That is, we consider the value of the probability density at evenly spaced spatial grid points $P_j(t) = P(j \delta n, t)$, where $\delta n = N/M$, M being an integer that determines the grid size. Furthermore, for the boundary condition of direct interest to us here, namely, absorption at each end of the interval, we have $P_0(t) = 0 = P_M(t)$. Thus, there are $M-1$ “live” independent variables: $P_1(t), P_2(t), \dots, P_{M-1}(t)$. These obey ODEs with the basic structure $\dot{P}_j = f_j(P_{j-1}, P_j, P_{j+1})$, where, as indicated, f_j depends only (linearly) on P_j and its two nearest neighbors.

Thus, we have a closed set of linear ODEs for $P_1 \dots P_{M-1}$, which we have chosen to integrate via a fourth-order Runge–Kutta scheme.³¹

The calculations of interest in the present work begin from a delta function initial condition, i.e., $\delta(n-n_0)$. To numerically compute the evolution of such an initial distribution using the 1-D finite-difference algorithm just described, we begin with a very narrow unit-normalized Gaussian. Its precise width influences only extremely short-time dynamics, but has no effect on quantities relevant to the translocation dynamics (e.g., any of the plots in Figs. 3 and 4).

Our immediate goal was to find a value of D and a value of F such that, when these were input into the 1-D Smoluchowski equation (4) with Sung–Park potential $V(n)$ [Eq. (5)], the best possible fit to the 3-D simulation data was obtained. Using the extraction procedure described in the previous section as a guide, we arrived, following minor empirical adjustments, at the values of $D=0.0135$ and $F=0.8$, which generated *all* the 1-D probability density evolution curves shown in Figs. 3 and 4. Considering the significant reduction in complexity involved, it is somewhat striking that a 1-D Smoluchowski model of the translocation coordinate dynamics describes the full 3-D system (consisting of $3N$ mechanical degrees of freedom) so well.

IV. TRANSLOCATION TIMES

Given the high degree of success found in representing the translocation dynamics of the 3-D N -monomer chain by a 1-D Smoluchowski equation it is not surprising that the mean first passage time (the integral of the survival probability from $t=0$ to $t=\infty$) calculated via 3-D and 1-D models agrees well for all chain lengths studied. Results are shown in Fig. 11. Three comments are appropriate. First, note that there is a second set of data points on the curve, corresponding to the “average survival time” T , which is defined operationally as

$$T(N) \equiv \frac{1}{A} \sum_{i=1}^A T_N^i, \quad (18)$$

where T_N^i is the survival time of the i th DMC run for a given polymer length N , the survival time for a given run being the time needed for all monomers of the polymer to thread from the *cis* to the *trans* side or for the polymer chain to completely retract to the *cis* side. It can be shown (cf. the Appendix) that, under conditions fulfilled in the present simulations, the mean first passage time is *equal* to the average survival time T , in the limit of infinite sampling. The small discrepancies between the two measures of survival time that are apparent in the simulation data presented in Fig. 11 can be attributed to statistical error inherent in the modest sample sizes utilized.

Second, note that the scaling of survival time with polymer length is linear. This is a consequence of (1) the domination of the linear potential ramp term in the Sung–Park potential, and (2) the fact that the diffusion constant D is approximately *independent* of the polymer chain length, consistent with arguments put forth by Muthukumar.⁷

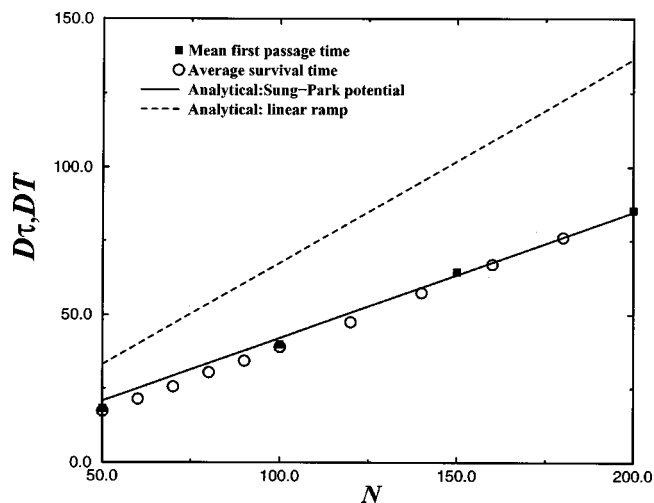


FIG. 11. The 3-D DMC simulation results of the average survival time T and the mean first passage time τ vs the polymer length N . The circles represent the results of T vs N obtained via Eq. (18). The squares represent the results of τ vs N obtained via Eq. (6). Shown via a straight line is the mean first passage time computed via the 1-D Smoluchowski equation model using the full Sung–Park potential (with parameter values $D=0.0135$, $F=0.8$) and double-absorbing boundary conditions; see the text for details. For a comparison, the dashed line shows the prediction obtained from the 1-D Smoluchowski equation model when only the linear term in the Sung–Park potential is retained [cf. Eq. (12)].

Finally, we stress that solid line in Fig. 11, which matches the 3-D DMC simulation data nicely, is based on the *full* Sung–Park potential, Eq. (5), including the conformational entropy term, with double-absorption boundary conditions. As discussed in Sec. III B, the mean first passage time resulting from 1-D Smoluchowski dynamics with these boundary conditions can be conveniently calculated for any potential $V(n)$ via the quadrature formula (7). This was done for the full Sung–Park potential to obtain the solid line in Fig. 11. For comparison, we also show in Fig. 11, via the dashed line, the result for the mean first passage time obtained by retaining only the linear term in the Sung–Park potential. As was noted in Sec. III B, for a linear potential ramp and double-absorption boundary conditions, this quantity is given by formula (12), which predicts linear scaling with polymer length. (In fact, for the parameters relevant in the present simulations, the shift constant C is very small and can be neglected.) Thus, we see that the entropic term in the Sung–Park potential does play some role in the quantitative details of the translocation, and that by including it, along with the proper boundary conditions, a virtually quantitative description of this translocation dynamics can be obtained via the 1-D Smoluchowski equation model described in Sec. III.

V. DISCUSSION AND CONCLUSIONS

In this paper we have presented results of 3-D Dynamic Monte Carlo (DMC) simulations of driven polymer transport through a cylindrical hole in a planar slab. In particular, a constant force was applied to monomers inside the hole. This system serves as a simple model for an important biophysical problem, namely, translocation of a charged biopolymer (e.g., single-stranded DNA or RNA) through an aqueous

pore in a cell or artificial membrane upon application of a *dc* electric field using microelectrode techniques. Of course, many features of the biological system that motivates our study have been suppressed in this minimalist model. The biopolymer is represented as a linear homopolymer chain. All chemical details of, say, the nucleotides of DNA have been ignored. Furthermore, as was briefly noted in Sec. II, the aqueous pores in biological cell walls are generated by specialized protein molecules that insert into the lipid bilayer membrane. As the biopolymer passes through such a pore, its monomers (nucleotides in the case of DNA/RNA) interacts strongly with the amino acids of the channel protein that line the pore wall. These interactions must depend on electrostatic and chemical details of both the channel protein and the nucleotide. Finally, electrostatic forces are much more complicated in real biological systems. In particular, there are mobile electrolyte ions in the aqueous regions. To treat these ions dynamically, on the same footing as the monomers of the polymer chain, would be very difficult from the perspective of current computer capabilities. Thus, in this initial study, we have assumed that they simply screen charges in the polymer chain (polyelectrolyte) so as to generate short-range intermonomer repulsions. Even the latter have been suppressed for simplicity in the simulations described in the present study, but, being of short-range character, they could be included within the computational framework employed here without difficulty.²³ A second important consequence of electrolyte screening is that when a voltage is applied across the cell membrane (e.g., via microelectrode techniques), the electric field thus established is essentially constant across the bilayer and zero outside it (due to polarization of the electrolyte clouds). This enables us, to a first approximation, to regard the force on each charged monomer of the polymer as constant inside the membrane (pore) and zero outside.

Despite its obvious oversimplifications, the model utilized in this work represents a step up in complexity and realism over previous theoretical analyses of electric field-driven polymer translocation through biological pores, which have been based on idealized 1-D models. These previous attempts have invoked a stochastic kinetic equation for the “translocation coordinate,” i.e., the number of monomers that have passed to the *trans* side of the membrane. Part of the motivation for the present study has been to calibrate these 1-D theories. Thus, we extracted from our 3-D simulations (involving $3N$ spatial degrees of freedom for a polymer composed of N monomers) the time evolution of the translocation coordinate. We found that, indeed, for a given polymer chain length, this probability distribution was well described for all times by a 1-D Smoluchowski equation of the type first proposed by Sung and Park.⁶ Their 1-D model contains two adjustable parameters (at a fixed temperature), namely, the linear driving force F and the effective diffusion constant D . A particularly interesting result of the present study is that the *same* value of F and the *same* value of D fit the 3-D simulation data for all chain lengths considered. The fact that the same F applies to all chain lengths suggests that this quantity can be approximately identified with the constant force field (characterized by strength constant k) applied across the channel in the 3-D simulation. The fact that

the same D value is appropriate for all chain lengths supports the contention of Muthukumar⁷ that this quantity is connected with the rate constant for attempted shifts of the translocation coordinate by ± 1 , which is furthermore assumed to be a local property, i.e., independent of how many monomers are attached to the parts of the polymer chain that “flip around” in the bulk solution on either side of the channel.

Future work will focus on several outstanding problems. First, in the present simulations, we avoided the problem of how the polymer chain “finds the pore,” i.e., diffusion toward the channel mouth. Such questions can be addressed by the methodology developed herein. Indeed, recent experimental work by Kasianowicz *et al.*³² indicates that there are unresolved questions associated with this issue. The experimentally observed rates of entry from the *cis* versus *trans* sides are different, which reflects in part the asymmetry in the structure of the α -hemolysin protein channel utilized in the experimental studies (and not accounted for in the present simulations).

Furthermore, in order to achieve more chemical realism in the model, we would like to add some distinguishing features of different monomers. For example, in the case of single-stranded DNA/RNA, the monomers are nucleotides (C, G, A, T for DNA) that differ in shape, charge distribution, etc. A more realistic pore shape and charge distribution characterizing the pore lining parts of the channel protein would also be useful.

Finally, in order to be able to accurately simulate translocation events in biological systems, a proper treatment of the electrostatic interactions should be attempted. As noted above, this is difficult, because there are, in fact, many mobile electrolyte ions in the aqueous solution. An intermediate level of description would treat the polymer as a “macroion,” and the electrolyte ions as a continuum probability density that can be determined (assuming the electrolyte ions equilibrate rapidly with each change in the polymer configuration) by solving the Poisson–Boltzmann equation³³ “on the fly.” Thus, many steps lie ahead in the quest for realistic simulations of these important processes.

ACKNOWLEDGMENTS

This work was supported in part by National Science Foundation Grant No. CHE-9633561. Computations presented here were carried out at the University of Pittsburgh’s Center for Molecular and Materials Science.

APPENDIX: EQUIVALENCE OF MEAN FIRST PASSAGE AND AVERAGE TRANSLOCATION TIME

Consider dynamics in a 1-D region $0 < n < N$. We do not assume that the kinetics is governed by the Smoluchowski equation, but only that “mass conservation” holds (which is the case for our translocation process). If $P(n, t)$ is the probability density at time t [normalized such that $\int_0^N dn P(n, 0) = 1$], this is the statement that

$$\partial P(n, t) / \partial t = -\partial j(n, t) / \partial n, \quad (\text{A1})$$

where $j(n, t)$ is the flux of particles³⁰ at position n and time t . That is, if there are \mathcal{N} particles in the box at $t=0$, then

$\mathcal{N}j(n,t)$ is the number of particles per unit time moving, say, to the right, through point n . Integration over the box region gives

$$\partial p_{\text{surv}}(t)/\partial t = -J(t), \quad (\text{A2})$$

where $p_{\text{surv}}(t) \equiv \int_0^N dn P(n,t)$ is the survival probability, and $J(t) \equiv j(N,t) - j(0,t)$. That is, $\mathcal{N}J(t)$ is the number of particles that exit the boundaries at $n=0$ and $n=N$ per unit time. In the case of direct interest to us, this exit is *permanent*, i.e., $\mathcal{N}J(t)$ is the rate of particle absorption at the two boundaries. Note that, since $p_{\text{surv}}(0)=1$ and $p_{\text{surv}}(\infty)=0$, Eq. (A2) implies that $\int_0^\infty dt J(t)=1$. Also note that $\mathcal{N}J(t)dt$ is the number of particles that survive to time t (i.e., are eliminated from the system in the interval $[t, t+dt]$). Thus, the average survival time is given by

$$T \equiv \int_0^\infty dt t \mathcal{N}J(t) / \int_0^\infty dt \mathcal{N}J(t) = \int_0^\infty dt t J(t). \quad (\text{A3})$$

Note that when this quantity is evaluated by discrete particle simulation, it is given by Eq. (18) in the text (in the limit of an infinitely large simulation sample).

Now we show that the mean first passage time, $\tau \equiv \int_0^\infty dt p_{\text{surv}}(t)$ is *equal* to the average survival time T , provided that $tp_{\text{surv}}(t) \rightarrow 0$ as $t \rightarrow \infty$. Simply integrate by parts:

$$\int_0^\infty dt t J(t) = -tp_{\text{surv}}(t)|_0^\infty + \int_0^\infty dt p_{\text{surv}}(t). \quad (\text{A4})$$

The surface term vanishes when the condition just noted holds, and thus $T=\tau$. Indeed, if $P(n,t)$ evolves according to a Smoluchowski equation, then $p_{\text{surv}}(t)$ is a sum of decaying exponentials,²⁹ so this condition is guaranteed to be satisfied. For the case of 3-D translocation dynamics, the time evolution of the translocation coordinate does not precisely satisfy a 1-D Smoluchowski equation, but does so to respectable accuracy. In any case, we have checked numerically that for the systems studied in this work $p_{\text{surv}}(t)$ falls rapidly to zero as $t \rightarrow \infty$, much faster than t^{-1} , thus ensuring $T=\tau$.

¹I. Szabo, G. Bathori, F. Tombola, M. Brini, A. Coppola, and M. Zoratti, *J. Biol. Chem.* **272**, 25275 (1997).

²I. Szabo, G. Bathori, F. Tombola, A. Coppola, I. Schemehl, M. Brini, A. Ghazi, V. De Pinto, and M. Zoratti, *FASEB J.* **12**, 495 (1998).

³B. Hanss, E. Leal-Pinto, L. A. Bruggeman, T. D. Copeland, and P. E.

Klotman, *Proc. Natl. Acad. Sci. U.S.A.* **95**, 1921 (1998).

⁴M. Akeson, D. Branton, J. J. Kasianowicz, E. Brandin, and D. W. Deamer, *Biophys. J.* **77**, 3227 (1999).

⁵J. J. Kasianowicz, E. Brandin, D. Branton, and D. W. Deamer, *Proc. Natl. Acad. Sci. U.S.A.* **93**, 13770 (1996).

⁶W. Sung and P. J. Park, *Phys. Rev. Lett.* **77**, 783 (1996).

⁷M. Muthukumar, *J. Chem. Phys.* **111**, 10371 (1999).

⁸D. K. Lubensky and D. R. Nelson, *Biophys. J.* **77**, 1824 (1999).

⁹In very recent work, Muthukumar¹⁰ has also performed DMC simulations on a related problem, namely translocation of a confined polymer through a hole in a spherical cavity.

¹⁰M. Muthukumar, *Phys. Rev. Lett.* **86**, 3188 (2001).

¹¹E. A. Di Marzio and A. J. Mandell, *J. Chem. Phys.* **107**, 5510 (1997).

¹²A. Baumgärtner and J. Skolnick, *Phys. Rev. Lett.* **74**, 2142 (1995).

¹³L. D. Simon, *Proc. Natl. Acad. Sci. U.S.A.* **69**, 907 (1972).

¹⁴U. K. Kaemmler and M. Favre, *J. Mol. Biol.* **80**, 575 (1973).

¹⁵Y.-B. Chung and D. C. Hinkle, *J. Mol. Biol.* **216**, 911 (1990).

¹⁶D. Kaiser, M. Syvanen, and T. Masuda, *J. Mol. Biol.* **91**, 175 (1975).

¹⁷I. Genes, C. H. Waddell, and J. King, *J. Mol. Biol.* **80**, 669 (1973).

¹⁸G. Pruss, R. N. Goldstein, and R. Calendar, *Proc. Natl. Acad. Sci. U.S.A.* **71**, 2367 (1974).

¹⁹S. M. Simon, C. S. Peskin, and G. F. Oster, *Proc. Natl. Acad. Sci. U.S.A.* **89**, 3770 (1992); C. S. Peskin, G. M. Odell, and G. F. Oster, *Biophys. J.* **65**, 316 (1993).

²⁰A. Baumgärtner and K. Binder, *J. Chem. Phys.* **71**, 2541 (1979).

²¹A. Baumgärtner, *J. Chem. Phys.* **72**, 871 (1980).

²²In biological systems, the two sides of a membrane may have different chemical/geometric characteristics, and are often distinguished using the terms *cis* and *trans* (Refs. 5 and 32). In the present work, on the other hand, there is no intrinsic difference between the two sides of the wall, so the labels *cis* and *trans* are somewhat arbitrary.

²³S. Tsonchev, R. D. Coalson, S.-S. Chern, and A. Duncan, *J. Chem. Phys.* **113**, 8381 (2000).

²⁴K. Binder and D. W. Heermann, *Monte Carlo Simulation in Statistical Physics* (Springer-Verlag, New York, 1988).

²⁵A. Kolinski, J. Skolnick, and R. Yaris, *J. Chem. Phys.* **86**, 7164 (1987).

²⁶See, for example, M. Doi and S. F. Edwards, *The Theory of Polymer Dynamics* (Clarendon, Oxford, 1986).

²⁷D. Bratko and K. A. Dawson, *J. Chem. Phys.* **99**, 5352 (1993).

²⁸A. Szabo, K. Schulten, and Z. Schulten, *J. Chem. Phys.* **72**, 4350 (1980).

²⁹H. Risken, *The Fokker-Planck Equation* (Springer-Verlag, Berlin, 1984); N. G. van Kampen, *Stochastic Processes in Physics and Chemistry*, 2nd ed. (North-Holland, Amsterdam, 1992).

³⁰In the context of the translocation problem under study here, "particle" is shorthand for a replica of the polymer system with a specified translocation coordinate n at time t .

³¹W. H. Press, B. P. Flannery, S. A. Teukolsky, and W. T. Vetterling, *Numerical Recipes* (Cambridge University Press, New York, 1986).

³²S. E. Henrickson, M. Misakian, B. Roberson, and J. L. Kasianowicz, *Phys. Rev. Lett.* **85**, 3057 (2000).

³³R. D. Coalson and T. L. Beck, *Encyclopedia of Computational Chemistry*, edited by P. von Rague Schleyer, New York, NY, 1998, Vol. 3, pp. 2086–2100.